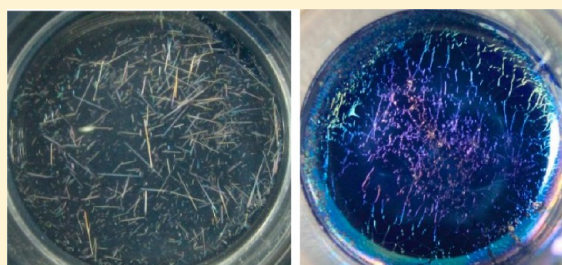


Unusual Enrichment and Assembly of TiO<sub>2</sub> Nanocrystals at Water/Hydrophobic Interfaces in a Pure Inorganic PhaseGuolei Xiang,<sup>†,‡</sup> Yong Long,<sup>†</sup> Jie He,<sup>†</sup> Biao Xu,<sup>†</sup> Haitao Liu,<sup>\*,‡</sup> and Xun Wang<sup>\*,†</sup><sup>†</sup>Department of Chemistry, Tsinghua University, Beijing 100084, China<sup>‡</sup>Department of Chemistry, University of Pittsburgh, Pittsburgh, Pennsylvania 15260, United States

## S Supporting Information

**ABSTRACT:** We report an unusual enrichment and assembly of TiO<sub>2</sub> nanocrystals at water/hydrophobic interfaces through oxidative hydrolysis of TiCl<sub>3</sub> in water. The assembly is a spontaneous process that involves on-water inorganic reaction and assembly in the absence of any organic phases. In this process, TiO<sub>2</sub> nanoparticles are preferentially produced at water/hydrophobic interfaces. When the surface tension of the aqueous phase is above a critical value, ca. 25–35 mN m<sup>−1</sup>, these TiO<sub>2</sub> nanocrystals can spontaneously accumulate at water/air interfaces to produce macroscopic sized sheets and tubes.



## 1. INTRODUCTION

A large body of literature has shown that water/hydrophobic interfaces possess unusual properties. For example, it is known that water/air and water/oil interfaces are negatively charged. Although the origin of these interfacial charges is still hotly debated, most studies have attributed it to the spontaneous interfacial accumulation of OH<sup>−</sup> or carboxylates.<sup>1–6</sup> In a similar vein, soft halogen anions in aqueous solutions are also known to be enhanced at air/water interfaces.<sup>7–10</sup> Sharpless and co-workers reported that certain organic reactions could be significantly accelerated, in some cases, by more than 100 times, by introducing macroscopic phase boundaries between water and the insoluble hydrophobic reactants.<sup>11</sup> Although the mechanism of the enhanced reactivity is largely unknown, experimental evidence suggests that it is likely related to the unique environments of the water/hydrophobic phase boundaries. Parallel to these studies, interfacial assembly of nanostructures at liquid/air and liquid/liquid interfaces has also attracted a lot of attention. Such processes rely on surface tension to pattern and assemble nano- and micrometer-scale materials into ordered macroscopic structures, like supercrystals, superlattices, and photonic crystals.<sup>12–24</sup> In these processes, the driving forces usually come from the hydrophobic interactions of surfactants that generate phase separation at interfaces.<sup>25,26</sup>

Herein we report an unusual enrichment and assembly result of TiO<sub>2</sub> nanocrystals at water/hydrophobic interfaces in the absence of any surfactants. We show that TiO<sub>2</sub> nanocrystals formed from TiCl<sub>3</sub> by oxidative hydrolysis can spontaneously accumulate at water/hydrophobic interfaces to form macroscopic sheets and tubes.

## 2. EXPERIMENTAL SECTION

**2.1. Interface Reactions.** **2.1.1. Surface Reactions at Air/Water Interfaces.** Reaction at Room Temperature (~20 °C). In a typical

reaction at room temperature (~20 °C), 0.3 mL of TiCl<sub>3</sub> solution was mixed with 30 mL of deionized water in a beaker and sealed using plastic wrap to prevent water evaporation and dust contamination from air. Then the solution was put in a hood for 2 days. After reaction, a layer of sheets floated on the surface of water.

**Reaction at 80 °C.** The reaction rates can be accelerated by increasing reaction temperatures. To prepare sheets, 0.5 mL of TiCl<sub>3</sub> solution was mixed with 30 mL of deionized water in a beaker and sealed using plastic wrap and then was put in an oven or water bath for 1 h. To prepare tubes, the difference is to reduce the amount of TiCl<sub>3</sub> solution to 0.1 mL.

**2.1.2. Reactions at Water/Organic Solvent Interfaces.** Oleic acid (OA) and *o*-dichlorobenzene (ODB) were used to create the upper and lower interfaces relative to water.

In the case of oleic acid (density, 0.89 g mL<sup>−1</sup>), 0.3 mL of TiCl<sub>3</sub> solution was mixed with 30 mL of deionized water in a beaker, and then 15 mL of OA was added. After being sealed with plastic wrap, the solution was put in an oven at 80 °C for 1 h. After reaction, a layer of sheets formed at the interface.

In the case of the lower interface, 20 mL of *o*-dichlorobenzene (density, 1.30 g mL<sup>−1</sup>) was first added in a round-bottom flask, and then TiCl<sub>3</sub> solution (0.3 mL in 30 mL of DI water) was added until overflow. After sealed with a plug, the solution was heated in a water bath at 80 °C for 1 h. After reaction, the products accumulated at the interface.

**2.1.3. Reaction Using H<sub>2</sub>O<sub>2</sub> as the Oxidant.** To test the difference between Ti<sup>4+</sup> and Ti<sup>3+</sup>, 0.05 mL of H<sub>2</sub>O<sub>2</sub> (30%) was added in TiCl<sub>3</sub> solution to oxidized Ti<sup>3+</sup> into Ti<sup>4+</sup>. After reaction at 80 °C for 1 h, only yellow precipitates were obtained.

**2.1.4. Effect of Surface Tension.** To check the roles of surface tensions of solvents in the spontaneous interface reactions and enrichment of TiO<sub>2</sub>, we changed the surface tensions of water by introducing one of the following three organic solvents: dimethylformamide (DMF), acetonitrile, and ethanol (EtOH). By keeping constant amounts of TiCl<sub>3</sub> solution (0.3 mL) and solvent volumes

Received: September 26, 2013

Revised: December 3, 2013

Published: January 2, 2014

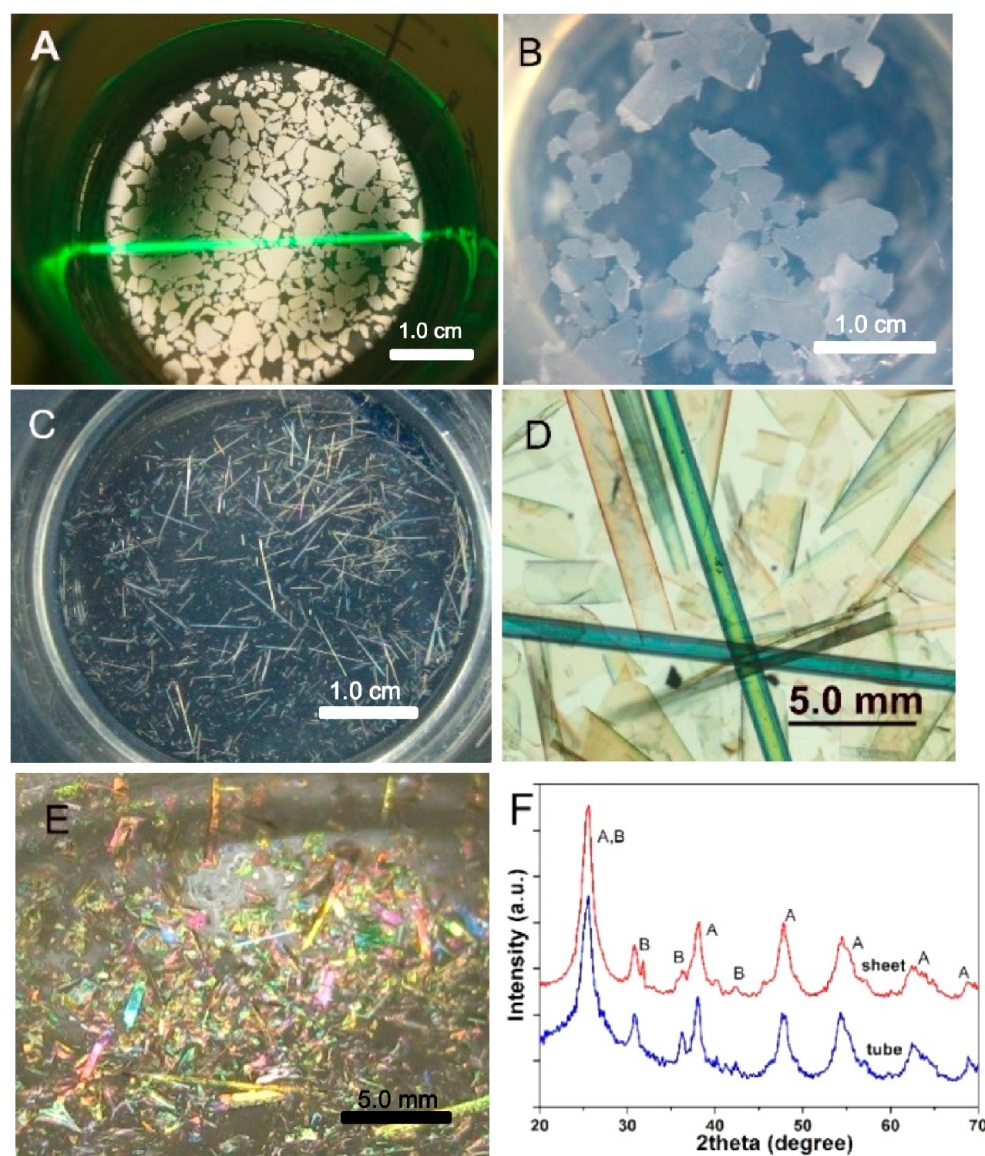


**Figure 1.** Enrichment and assembly results of  $\text{TiO}_2$  nanocrystals at air/water interfaces. (A) Image showing the hydrolysis result of  $\text{TiCl}_3$  at room temperature ( $20^\circ\text{C}$ ) for 2 days. (B) Macrosheets floating on water after 1 h reaction at  $80^\circ\text{C}$ . (C) Macrotubes formed after 1 h reaction at  $80^\circ\text{C}$ . (D) Optical microscopy image of macrotubes showing completely and partly rolled tubes. (E) Image of chromatic macrotubes after drying. (F) XRD patterns of sheets (top) and tubes (down), both of which are composed of anatase (A) and brookite (B). (A)–(C) show the top views of the beakers.

(30 mL), a series of experiments were conducted at  $80^\circ\text{C}$  in solvents composed of water and organic phases with different ratios. The critical ratios of volumes at which the surface products nearly disappeared were  $\text{DMF:H}_2\text{O} = 22\text{ mL}:8\text{ mL}$ ,  $\text{acetonitrile:H}_2\text{O} = 14\text{ mL}:16\text{ mL}$ , and  $\text{EtOH:H}_2\text{O} = 16\text{ mL}:14\text{ mL}$ .

**2.1.5. Eliminating the Contamination of Hydrocarbons.** Adsorption of hydrocarbon molecules from the environment can decrease the hydrophilicity of a surface. We eliminated this possibility with two control experiments where we conducted the reaction under the irradiation of a 300 W UV lamp (wavelength 365 nm) and irradiated the sheets on water for 15 h. Both procedures are known to remove adsorbed hydrocarbon on photocatalytic  $\text{TiO}_2$ ; however, in both cases, the sheets could remain on the surfaces, indicating that the floating of nanocrystals is not due to hydrocarbon adsorption.

**2.2. Characterizations.** Phases of the sheets and tubes were determined on a Bruker D8 Advance X-ray diffractometer using  $\text{Cu K}\alpha$  radiation ( $\lambda = 0.15418\text{ nm}$ ). The products were picked up from water using glass slides and were scanned directly. Surface tensions of the mixed solvents at critical points were measured through ring method.

Briefly, the solvents were heated to  $80^\circ\text{C}$  in a water bath, and then the surface tension was measured by pulling a platinum ring out of the surface. Contact angle of water on the  $\text{TiO}_2$  sheet was measured using a VCA-OPTIMA contact angle tester. The sheets floating on water was picked up using a glass slide. Surface structures of the sheets were characterized on a JEOL JSM-6700F scanning electron microscope (SEM). The sheets floating on water was picked up using a Si wafer.

### 3. RESULTS

#### 3.1. Spontaneous Assembly at Air/Water Interfaces.

In a typical experiment, 0.3 mL of aqueous  $\text{TiCl}_3$  solution was dissolved in 30 mL of deionized water and left in air at  $20^\circ\text{C}$  for 2 days. During the reaction,  $\text{Ti}^{3+}$  was slowly oxidized by  $\text{O}_2$  into  $\text{TiO}^{2+}$ , which further hydrolyzed to produce  $\text{TiO}_2$  nanocrystals. The presence of  $\text{TiO}_2$  colloids in the bulk solution was verified by the Tyndall effect (Figure 1A). Surprisingly, we also observed sheet-like structures floating on the air/water interface. By increasing the reaction temperature



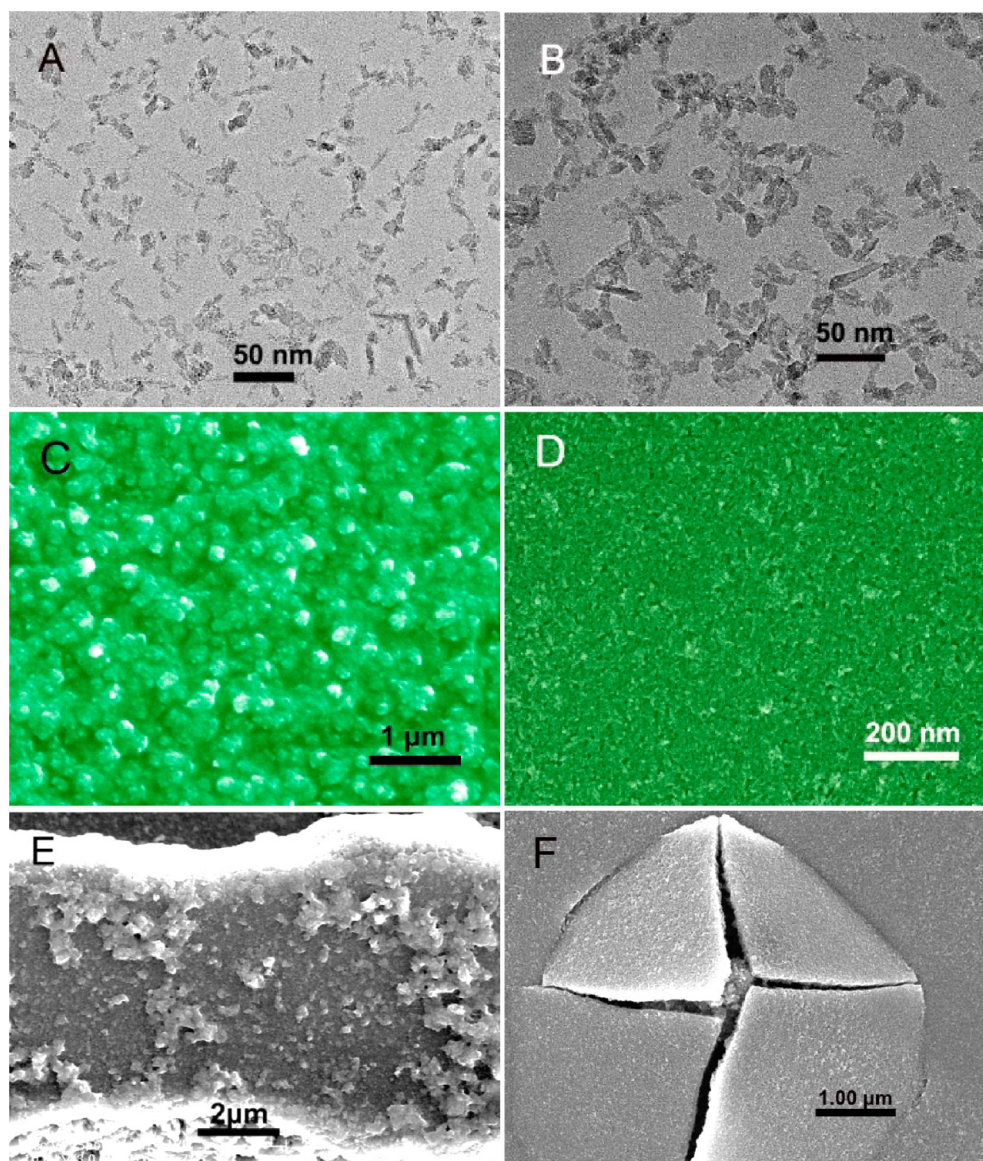


**Figure 2.** Microstructures of TiO<sub>2</sub> macrosheets and macrotubes. (A, C, E) TEM and SEM images of sheets. (B, D, F) TEM and SEM images of tubes.

to 80 °C, the rates of reaction and surface assembly were accelerated, and different macrostructures could also be obtained by adjusting the amount of TiCl<sub>3</sub>. Sheets floating on water were the major products when the amount of TiCl<sub>3</sub> was over 0.3 mL in 30 mL of water at 80 °C (Figure 1B); chromatic macrotubes were obtained by decreasing the amount of TiCl<sub>3</sub> to 0.1 mL (Figure 1C and Figure S1). Different from the sheets, these tubes would sink into water after formation rather than floated on the surfaces. Structures of the tubes can be resolved by an optical microscope; both complete tubes and partly rolled sheets are present (Figure 1D), and some of the tubes have multilayer structures (Figure S1). These observations suggest that these macrotubes are likely formed in a two-step manner: formation of sheets via interfacial assembly and subsequent rolling-up into tubes. Interestingly, the colors of the tubes were maintained even after drying in air (Figure 1E), pointing to their potential applications as chromatic materials. Despite the difference in morphologies, both the sheets and tubes are made of anatase and brookite TiO<sub>2</sub> as shown by X-ray diffraction (XRD, Figure 1F).

**3.2. Microstructure Analysis.** The assembled macroscale structures are composed of TiO<sub>2</sub> nanocrystals linked via weak interparticle interactions. Both the sheets and tubes can be destroyed by ultrasonication in ethanol to produce irregularly shaped TiO<sub>2</sub> nanoparticles as observed by transmission electron microscopy (TEM) images (Figure 2A,B). When observed under a scanning electron microscope (SEM, Figure 2C,D), the surface roughness of the sheets was found to be higher than that of the tubes. These results suggest that the sheets and tubes are assembled from TiO<sub>2</sub> nanoparticles that result from the oxidative hydrolysis of TiCl<sub>3</sub>. As characterized by high-resolution scanning electron microscopy (HRSEM, Figure S2A), the sheets and tubes are microporous due to the random assembly of nanoparticles.

Apart from surface roughness, the sheets and tubes also have different thicknesses as shown by the side view SEM images in Figure 2E,F. The thickness of a typical sheet is about 6 μm compared to about 500 nm for tubes. Such differences in the surface roughness and thickness were due to the different growth conditions of tubes and sheets. Because the sheets are

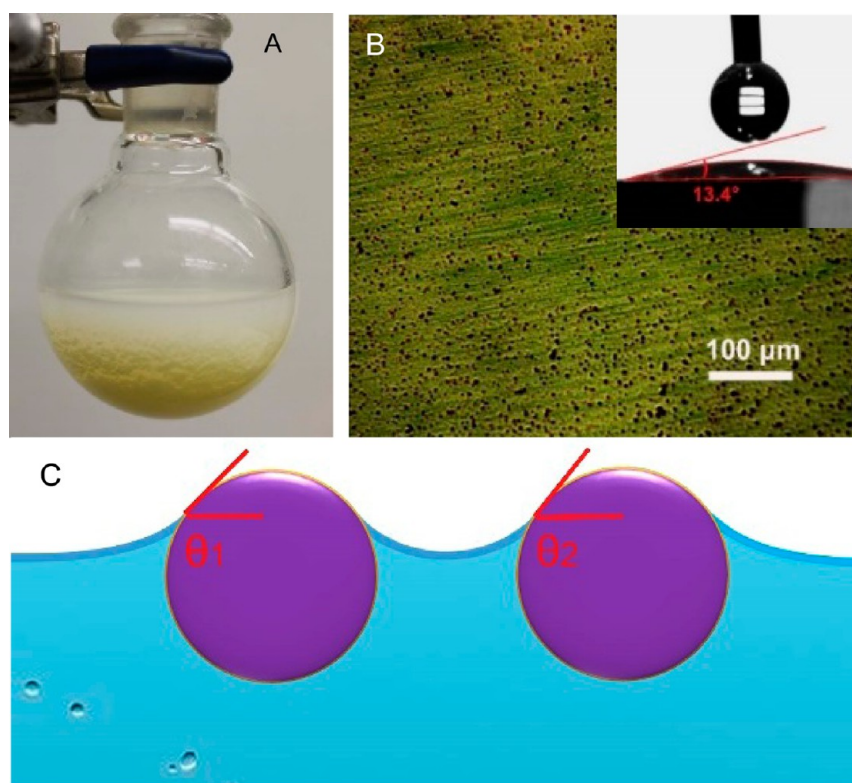


**Figure 3.** Mechanism analysis of the spontaneous interfacial phenomena. (A) Reaction results by introducing  $\text{H}_2\text{O}_2$  in  $\text{TiCl}_3$  aqueous solution. (B) Optical microscope image of a sheet and the contact angle of water on it ( $13.4^\circ$ ), showing hydrophilicity. (C) Scheme of attractive lateral immersion forces between adjacent hydrophilic particles floating on water surfaces.

obtained at a higher  $\text{TiCl}_3$  concentration, faster growth rates of  $\text{TiO}_2$  can be expected, and more nanoparticles are generated during the same reaction time. As a result, the sheets are thicker and rougher than the tubes. The chromatic character of the tubes is likely due to interference because the wall thickness of the tubes is similar to that of the wavelength of visible light. We did notice that the sheets could be chromatic when they were not too thick as shown in Figure S2B. Such chromatic sheets were typically formed during the first 15 min of the reaction and then evolved to produce the tubes and thicker sheets. At a low  $\text{TiCl}_3$  concentration, rolling-up is favored while at high  $\text{TiCl}_3$  concentration, sheets continue to grow thicker because of the sufficient supply of precursors. Although the detailed mechanism is not known, the fact that the tubes can only be obtained at above  $60^\circ\text{C}$  suggests that the surface features of water at higher temperatures could contribute to the formation of tubes.

**3.3. Spontaneous Assembly Results at Oil/Water Interfaces.** Such interfacial enrichment and assembly process are related to the in-situ generation of  $\text{TiO}_2$  nanocrystals and is not observed for preformed ones. To show this was the case, we collected the  $\text{TiO}_2$  sheets/tubes and destroyed them by ultrasonication. After keeping the nanocrystal suspensions at  $80^\circ\text{C}$  for 3 h, we observed no assembled  $\text{TiO}_2$  structure at air/water interface.

Additional experiments show that the air/water interface is not special for this reaction; the same phenomena can be reproduced at water/oil interfaces as well. For example, oleic acid (OA, Figure S3A) and *o*-dichlorobenzene (ODB, Figure S3B) were used to create the upper and lower water/hydrophobic interfaces relative to water. After reactions at  $80^\circ\text{C}$  for 1 h, in both cases,  $\text{TiO}_2$  sheet products appeared at the

interfaces, suggesting that the  $\text{TiO}_2$  products can always enrich around water/hydrophobic interfaces, independent of the nature of the hydrophobic phase as well as its location.

## 4. DISCUSSION

**4.1. Roles of Oxidative Hydrolysis of  $\text{TiCl}_3$ .** We propose that the interfacial enrichment and assembly of  $\text{TiO}_2$  nanocrystals are due to enhanced oxidative hydrolysis of  $\text{TiCl}_3$  at the water/hydrophobic interface and capturing of *in situ* formed  $\text{TiO}_2$  nanocrystals at the interface by surface tension. In our experiments, the  $\text{TiO}_2$  nanocrystals were produced by oxidation of  $\text{Ti}^{3+}$  by  $\text{O}_2$  to  $\text{TiO}^{2+}$ , followed by hydrolysis of  $\text{TiO}^{2+}$  to produce  $\text{TiO}_2$ . At least two mechanisms could result in an increase of reaction rate at the water/hydrophobic interface. First, because the concentration of  $\text{O}_2$  is much higher in air and organic solvent than in water, the concentration of  $\text{O}_2$  at the water/air interface and water/oil interface could be higher than that of bulk aqueous phase, leading to a faster oxidation of  $\text{TiCl}_3$ . Second, it has been suggested that  $\text{OH}^-$  ions spontaneously adsorb at water/hydrophobic interfaces; as a result, the local pH at the water/hydrophobic interface is higher than the bulk value. Such an effect could lead to enhanced hydrolysis of  $\text{TiO}^{2+}$  and production of  $\text{TiO}_2$  at the water/hydrophobic interface.

Our hypothesis was supported by several additional control experiments. For example, the present enrichment and assembly results can only be obtained by using  $\text{Ti}^{3+}$  precursors like  $\text{TiCl}_3$  or  $\text{Ti}_2(\text{SO}_4)_3$ , while using  $\text{Ti}^{4+}$  compounds (e.g.,  $\text{Ti}(\text{OCH}(\text{CH}_3)_2)_4$ ) only produced milky slurries of  $\text{TiO}_2$ . Similarly, if  $\text{H}_2\text{O}_2$  was used as an oxidation agent to oxidize  $\text{TiCl}_3$ , only yellow precipitates were obtained (Figure 3A). Together, these results indicate that interfacial oxidation is key



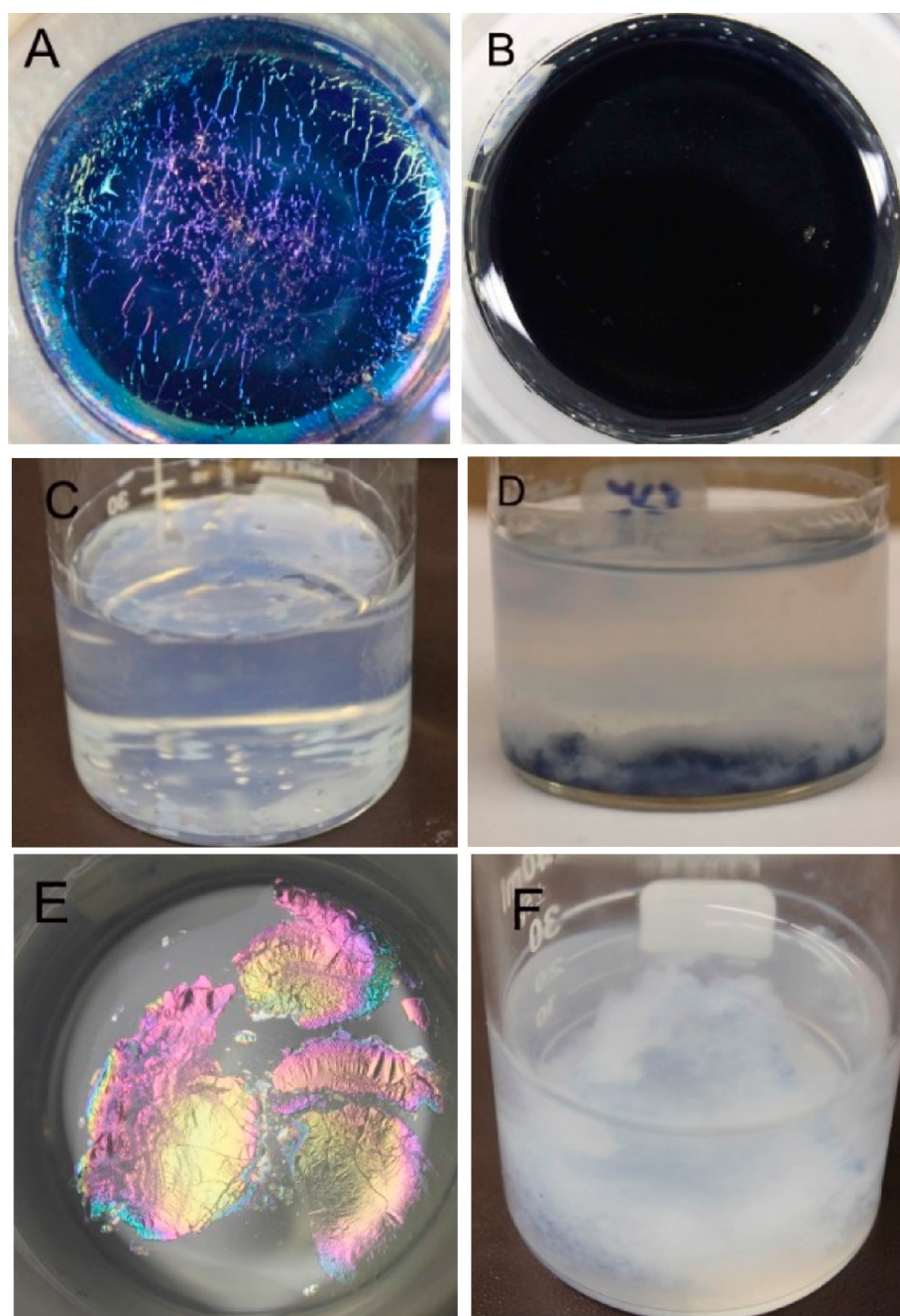


**Figure 4.** Solvent effects showing the roles of surface tensions on the interfacial enrichment and assembly. (A, B) Results in DMF,  $V(\text{DMF}):V(\text{H}_2\text{O}) = 10 \text{ mL}:20 \text{ mL}$  for (A) and  $23 \text{ mL}:7 \text{ mL}$  for (B). (C, D) Results in acetonitrile,  $V(\text{acetonitrile}):V(\text{H}_2\text{O}) = 10 \text{ mL}:20 \text{ mL}$  for (C) and  $15 \text{ mL}:15 \text{ mL}$  for (D). (E, F) Results in ethanol  $V(\text{EtOH}):V(\text{H}_2\text{O}) = 6 \text{ mL}:24 \text{ mL}$  for (E) and  $V(\text{EtOH}):V(\text{H}_2\text{O}) = 17 \text{ mL}:13 \text{ mL}$  for (F).

to the observed enrichment effect. This conclusion can be further confirmed by conducting the reaction in  $\text{O}_2$ -free conditions. In that case, the reaction produced almost no products on the air/water interface (Figure S4), indicating that the surface reaction and assembly were highly suppressed in the absence of  $\text{O}_2$ .

**4.2. Floating Analysis.** An intriguing question is the mechanism of the stabilization of  $\text{TiO}_2$  structures at the water/hydrophobic interface. Hydrophobic materials are known to “float” on water surface due to surface tension and hydrophobic interactions.<sup>27,28</sup> However, this is not the case for the present  $\text{TiO}_2$  structures: a clean  $\text{TiO}_2$  surface is hydrophilic and only becomes hydrophobic when contaminated by hydrocarbon.

However, our control experiments rule out this possibility (see Supporting Information for details). Indeed, when picked up by a glass substrate, the  $\text{TiO}_2$  sheets gave a water contact angle of  $13.4^\circ$ , indicating a highly hydrophilic nature (Figure 3B). On the other hand, an apparent fact is that the top surfaces of the sheets were not wetted by water, and the sheets will immediately sink if immersed in water. The results suggest that the hydrophilic sheets float on water surfaces in a metastable manner without being completely wetted by water. Certain hydrophilic particles (e.g.,  $\text{SiO}_2$  and  $\text{TiO}_2$ ) are known to remain on water surface when spread onto water from a suspension in alcohol.<sup>29–31</sup> These results show that hydrophilic structures assembled from nanoparticles can float on the surface

of water, and the floating is thought to originate from the collective motions of the hydrophilic particles. However, a detailed mechanism is still unknown.<sup>31</sup>

### 4.3. Roles of Surface Tensions on Assembly Results.

The assembly of hydrophilic  $\text{TiO}_2$  nanoparticles on water surface can be interpreted in terms of lateral immersion force, a capillary force driven by wetting.<sup>32,33</sup> When two hydrophilic particles are partly immersed on a liquid surface as shown in Figure 3C, the surface is deformed because of the effects of wetting. A lateral immersion force exists between the adjacent particles, attractive or repulsive depending on the signs of the meniscus slope angles  $\theta_1$  and  $\theta_2$  at the two contact lines: the capillary force is attractive when  $\sin \theta_1 \sin \theta_2 > 0$  and repulsive when  $\sin \theta_1 \sin \theta_2 < 0$ . For the present hydrophilic  $\text{TiO}_2$  particles protruding on water interface, both  $\theta_1$  and  $\theta_2$  are positive. As a result, an attractive lateral immersion forces will pull  $\text{TiO}_2$  nanoparticles together. This attractive lateral immersion force ( $F$ ) is proportional to the surface tension ( $\sigma$ ) of the liquid through eq 1:

$$F = k\sigma R^2 \quad (1)$$

where  $k$  is a constant and  $R$  is the radii of the particle. Equation 1 indicates that the assembly and stability of the sheet structure critically depend on the surface tension.

We found that surface tension indeed played a key role in this interfacial assembly process. We adjusted the surface tension of water by mixing it with other organic solvents. The results in the mixtures of water with dimethylformamide (DMF), acetonitrile, and ethanol (EtOH) (80 °C for 1 h) are shown in Figure 4. Although different organic solvents were introduced,  $\text{TiO}_2$  products could still accumulate at interfaces when their concentrations were low (Figures 4A,C,E). However, as the concentration of the organic solvent increased over a specific critical value, only  $\text{TiO}_2$  precipitates were obtained (Figures 4B,D,F). This fact indicates that the presence of larger amount of miscible organic solvents specifically suppresses interfacial assembly without affecting the overall hydrolytic reaction. By keeping the total volumes constant (30 mL), we determined the critical volume ratios of organic solvents to water through a series of experiments at 80 °C in water baths (Table 1 and Figure S5). Although the critical

**Table 1. Critical Ratios of Solvents to Water and Corresponding Surface Tensions at 80 °C ( $\sigma$ , mN m<sup>-1</sup>)**

	solvent		
	DMF	acetonitrile	EtOH
ratios <sup>a</sup>	22:8	14:16	16:14
surface tension	34.42	31.23	25.69

<sup>a</sup>The ratios are in volumes by keeping total volume constant at 30 mL.

concentrations vary significantly among different solvents, we find that at the critical concentrations these water/organic mixtures exhibit very similar surface tensions of ca. 25–35 mN m<sup>-1</sup>, which were measured through ring method at 80 °C. If the surface tension of the aqueous phase was higher than this range, we could consistently observe the aforementioned interfacial enrichment and assembly.

We found that the stability of an already assembled  $\text{TiO}_2$  sheet depends on the surface tension of the subphase as well. The  $\text{TiO}_2$  sheets prepared in pure water could stay afloat on water surface for tens of days. However, these sheets would soon break down when ethanol was introduced into the

subphase. This observation again suggests that the  $\text{TiO}_2$  sheets are dynamically assembled from small  $\text{TiO}_2$  nanocrystals by the lateral immersion force.

## 5. CONCLUSIONS

In summary, we have studied an unusual enrichment and assembly of  $\text{TiO}_2$  nanocrystals at water/hydrophobic interfaces to form sheets and tubes in the absence of any surfactants. Our results demonstrate a novel approach to self-assemble nano-scale objects to form macroscopic 2D and 3D structures. Work is underway to probe the detailed mechanism of the assembly and to control the morphology of the assembled products.

## ■ ASSOCIATED CONTENT

### Supporting Information

Experimental details and the results of control experiments. This material is available free of charge via the Internet at <http://pubs.acs.org>.

## ■ AUTHOR INFORMATION

### Corresponding Authors

\*E-mail [hliu@pitt.edu](mailto:hliu@pitt.edu) (H.L.).

\*E-mail [wangxun@mail.tsinghua.edu.cn](mailto:wangxun@mail.tsinghua.edu.cn) (X.W.).

### Notes

The authors declare no competing financial interest.

## ■ ACKNOWLEDGMENTS

This work was supported by the National Natural Science Foundation of China (91127040 and 21221062) and the State Key Project of Fundamental Research for Nanoscience and Nanotechnology (2011CB932402). H.L. acknowledges support from AFOSR (FA9550-13-1-0083) and ONR (N000141310575). G. L. Xiang acknowledges financial support by China Scholarship Council for his study in the University of Pittsburgh in 2013.

## ■ REFERENCES

- (1) Mishra, H.; Enami, S.; Nielsen, R. J.; Stewart, L. A.; Hoffmann, M. R.; Goddard, W. A.; Colussi, A. J. Bronsted basicity of the air-water interface. *Proc. Natl. Acad. Sci. U. S. A.* **2012**, *109*, 18679–18683.
- (2) Beattie, J. K.; Djerdjev, A. M. The pristine oil/water interface: surfactant-free hydroxide-charged emulsions. *Angew. Chem., Int. Ed.* **2004**, *43*, 3568–3571.
- (3) Roger, K.; Cabane, B. Why are hydrophobic/water interfaces negatively charged? *Angew. Chem., Int. Ed.* **2012**, *51*, 5625–5628.
- (4) Beattie, J. K.; Gray-Weale, A. Oil/water interface charged by hydroxide ions and deprotonated fatty acids: A comment. *Angew. Chem., Int. Ed.* **2012**, *51*, 12941–12942.
- (5) Roger, K.; Cabane, B. Uncontaminated hydrophobic/water interfaces are uncharged: A reply. *Angew. Chem., Int. Ed.* **2012**, *51*, 12943–12945.
- (6) Tian, C. S.; Shen, Y. R. Structure and charging of hydrophobic material/water interfaces studied by phase-sensitive sum-frequency vibrational spectroscopy. *Proc. Natl. Acad. Sci. U. S. A.* **2009**, *106*, 15148–15153.
- (7) Knipping, E. M.; Lakin, M. J.; Foster, K. L.; Jungwirth, P.; Tobias, D. J.; Gerber, R. B.; Dabdub, D.; Finlayson-Pitts, B. J. Experiments and simulations of ion-enhanced interfacial chemistry on aqueous NaCl aerosols. *Science* **2000**, *288*, 301–306.
- (8) Jungwirth, P.; Tobias, D. J. Molecular structure of salt solutions: A new view of the interface with implications for heterogeneous atmospheric chemistry. *J. Phys. Chem. B* **2001**, *105*, 10468–10472.
- (9) Laskin, A.; Gaspar, D. J.; Wang, W. H.; Hunt, S. W.; Cowin, J. P.; Colson, S. D.; Finlayson-Pitts, B. J. Reactions at interfaces as a source of sulfate formation in sea-salt particles. *Science* **2003**, *301*, 340–344.

- (10) Jungwirth, P.; Tobias, D. J. Specific ion effects at the air/water interface. *Chem. Rev.* **2006**, *106*, 1259–1281.
- (11) Narayan, S.; Muldoon, J.; Finn, M. G.; Fokin, V. V.; Kolb, H. C.; Sharpless, K. B. “On water”: Unique reactivity of organic compounds in aqueous suspension. *Angew. Chem., Int. Ed.* **2005**, *44*, 3275–3279.
- (12) Dong, A. G.; Chen, J.; Vora, P. M.; Kikkawa, J. M.; Murray, C. B. Binary nanocrystal superlattice membranes self-assembled at the liquid-air interface. *Nature* **2010**, *466*, 474–477.
- (13) Kalsin, A. M.; Fialkowski, M.; Paszewski, M.; Smoukov, S. K.; Bishop, K. J. M.; Grzybowski, B. A. Electrostatic self-assembly of binary nanoparticle crystals with a diamond-like lattice. *Science* **2006**, *312*, 420–424.
- (14) Zhang, Y. R.; Xu, Y. Z.; Xia, Y.; Huang, W.; Liu, F. A.; Yang, Y. C.; Li, Z. L. A novel strategy to assemble colloidal gold nanoparticles at the water-air interface by the vapor of formic acid. *J. Colloid Interface Sci.* **2011**, *359*, 536–541.
- (15) Beaman, D. K.; Robertson, E. J.; Richmond, G. L. Ordered polyelectrolyte assembly at the oil-water interface. *Proc. Natl. Acad. Sci. U. S. A.* **2012**, *109*, 3226–3231.
- (16) Talapin, D. V.; Shevchenko, E. V.; Bodnarchuk, M. I.; Ye, X. C.; Chen, J.; Murray, C. B. Quasicrystalline order in self-assembled binary nanoparticle superlattices. *Nature* **2009**, *461*, 964–967.
- (17) Smith, D. K.; Goodfellow, B.; Smilgies, D. M.; Korgel, B. A. Self-assembled simple hexagonal AB<sub>2</sub> binary nanocrystal superlattices: SEM, GISAXS, and defects. *J. Am. Chem. Soc.* **2009**, *131*, 3281–3290.
- (18) Gu, Z. Z.; Wang, D.; Mohwald, H. Self-assembly of microspheres at the air/water/air interface into free-standing colloidal crystal films. *Soft Matter* **2007**, *3*, 68–70.
- (19) Henzie, J.; Grunwald, M.; Widmer-Cooper, A.; Geissler, P. L.; Yang, P. Self-assembly of uniform polyhedral silver nanocrystals into densest packings and exotic superlattices. *Nat. Mater.* **2012**, *11*, 131–137.
- (20) Wang, J.; Wang, D. Y.; Sobal, N. S.; Giersig, M.; Jiang, M.; Mohwald, H. Stepwise directing of nanocrystals to self-assemble at water/oil interfaces. *Angew. Chem., Int. Ed.* **2006**, *45*, 7963–7966.
- (21) Shevchenko, E. V.; Talapin, D. V.; Kotov, N. A.; O'Brien, S.; Murray, C. B. Structural diversity in binary nanoparticle superlattices. *Nature* **2006**, *439*, 55–59.
- (22) Tao, A.; Sinsermsuksakul, P.; Yang, P. Tunable plasmonic lattices of silver nanocrystals. *Nat. Nanotechnol.* **2007**, *2*, 435–440.
- (23) Cote, L. J.; Kim, F.; Huang, J. X. Langmuir-Blodgett assembly of graphite oxide single layers. *J. Am. Chem. Soc.* **2009**, *131*, 1043–1049.
- (24) Ge, J. P.; Lee, H.; He, L.; Kim, J.; Lu, Z. D.; Kim, H.; Goebel, J.; Kwon, S.; Yin, Y. D. Magnetochromatic microspheres: Rotating photonic crystals. *J. Am. Chem. Soc.* **2009**, *131*, 15687–15694.
- (25) Bigioni, T. P.; Lin, X. M.; Nguyen, T. T.; Corwin, E. I.; Witten, T. A.; Jaeger, H. M. Kinetically driven self assembly of highly ordered nanoparticle monolayers. *Nat. Mater.* **2006**, *5*, 265–270.
- (26) Chandler, D. Interfaces and the driving force of hydrophobic assembly. *Nature* **2005**, *437*, 640–647.
- (27) Moore, F. G.; Richmond, G. L. Integration or segregation: How do molecules behave at oil/water interfaces? *Acc. Chem. Res.* **2008**, *41*, 739–748.
- (28) Larmour, I. A.; Saunders, G. C.; Bell, S. E. Sheets of large superhydrophobic metal particles self assembled on water by the Cheerios effect. *Angew. Chem., Int. Ed.* **2008**, *47*, 5043–5046.
- (29) Park, S.; Lee, H. B. Effect of pH on monolayer properties of colloidal silica particles at the air/water interface. *Colloid Polym. Sci.* **2012**, *290*, 445–455.
- (30) McNamee, C. E.; Yamamoto, S.; Butt, H. J.; Higashitani, K. A straightforward way to form close-packed TiO<sub>2</sub> particle monolayers at an air/water interface. *Langmuir* **2011**, *27*, 887–894.
- (31) Moon, G. D.; Lee, T. I.; Kim, B.; Chae, G.; Kim, J.; Kim, S.; Myoung, J. M.; Jeong, U. Assembled monolayers of hydrophilic particles on water surfaces. *ACS Nano* **2011**, *5*, 8600–8612.
- (32) Kralchevsky, P. A.; Nagayama, K. Capillary interactions between particles bound to interfaces, liquid films and biomembranes. *Adv. Colloid Interface Sci.* **2000**, *85*, 145–192.
- (33) Paunov, V. N.; Kralchevsky, P. A.; Denkov, N. D.; Nagayama, K. Lateral capillary forces between floating submillimeter particles. *J. Colloid Interface Sci.* **1993**, *157*, 100–112.